

Microsolvation of Hg and Hg²⁺: Energetics of Hg·H₂O, Hg²⁺·H₂O and HgOH⁺

Pavel Soldán,^{*,†} Edmond P. F. Lee,^{*,‡,§} and Timothy G. Wright^{*,||}

Department of Chemistry, University of Durham, South Road, Durham DH1 3LE, United Kingdom, Department of Applied Biology and Chemical Technology, Hong Kong Polytechnic University, Hung Hom, Hong Kong, Department of Chemistry, University of Southampton, Highfield, Southampton SO17 1BJ, United Kingdom, and Spectroscopy of Complexes and Radicals (SOCAR) Group, Department of Chemistry, School of Chemistry, Physics and Environmental Science, University of Sussex, Falmer, Brighton BN1 9QJ, United Kingdom

Received: June 14, 2002; In Final Form: July 19, 2002

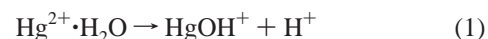
High-level ab initio and DFT calculations are employed to calculate the geometries of monosolvated Hg and Hg²⁺. In agreement with previous studies on M²⁺·H₂O species, we calculate the equilibrium geometry of the Hg²⁺·H₂O dicationic complex as having the Hg²⁺ interacting with the oxygen atom of water, but we find that the minimum energy geometry is nonplanar and attribute this to covalency. For Hg·H₂O, in contrast to many previous studies on neutral M·H₂O species, but in agreement with our previous studies, we find that the Hg atom prefers to be situated on the hydrogen end of the water molecule, in a C_s orientation. We rationalize this in terms of electron–electron repulsion. We calculate the energies of the lowest states of HgOH⁺ and conclude that the ground state is a bent, closed-shell ¹A' state, with a fair amount of covalency. CCSD(T) calculations employing very large basis sets, and employing the above geometries, allow us to calculate values for the interaction energies of Hg·H₂O (213 cm⁻¹) and Hg²⁺·H₂O (90 kcal mol⁻¹). In addition, the enthalpy of reaction for the process Hg²⁺ + H₂O → HgOH⁺ + H⁺ is calculated to be -40 kcal mol⁻¹ at the highest level of theory used herein. Finally, we conclude that the Hg²⁺·H₂O complex should be observable, but that care in its preparation is required.

I. Introduction

Mercury is a well-known contaminant of the lower troposphere,¹ being emitted from industrial processes,^{2,3} as well as from the vaporization of tooth fillings upon cremation of human bodies. It exists mainly in its elemental Hg⁰ form,^{4,5} but with significant amounts also present as reactive gaseous mercury (RGM).^{6,7} "Knowledge of the speciation of atmospheric [mercury] is crucial for predicting its deposition and understanding its bio-geochemical cycling."⁶ The cycling of mercury between water, air, and soil has been examined.⁸ In particular, recently, the dissolution of mercury into water droplets, and the agglomeration of mercury into ice have been shown to be of importance and have been implicated in the depletion of atmospheric mercury in the Antarctic Spring,⁹ and the oxidation of Hg in the Arctic troposphere.¹⁰

Mercury is also known to be extremely toxic to man. As such, its absorption into the body and its chemistry therein is of extreme importance. The deleterious effect of Hg is thought to stem from the formation of methylmercury, which affects the central nervous system. However, the hydrates of Hg are also of great importance. Although mercury forms Hg(I) and Hg(III)

compounds, and even Hg(0.33),¹¹ it is the Hg(II) compounds that are the most stable in solution and, hence, of the most interest. Mercury vapor (Hg⁰) is known to be a dangerous substance, with prolonged exposure leading to absorption and, owing to its long retention time, a build up in concentration in the body and so harmful effects. The primary interaction of a Hg atom with the human body is probably with a water molecule, leading eventually to solvation and absorption into the blood stream. Thus, the physicochemical characteristics of the 1:1 complex of Hg with H₂O and Hg²⁺ with H₂O are of fundamental interest. In this work, we address both of these systems, basing our methodology on our recent work on the corresponding cadmium compounds.¹² We present a high-level study of the neutral Hg·H₂O complex, the dicationic complex Hg²⁺·H₂O, and the reaction



which is considered to be a key step in the hydrolysis of the Hg²⁺ ion¹³

Previous studies on the Hg²⁺·H₂O species have formed part of a study of a number of hydrates of mercury. Those by Probst¹⁴ and by Sinha¹⁵ shall be referred to below. We also note that, in addition to our recent theoretical study,¹² combined theoretical and Raman studies of the hydration of the other Group IIb dications, Zn²⁺ and Cd²⁺, have been undertaken.^{16,17} Interestingly, in a matrix isolation study on Group IIb hydrides, Greene et al.¹⁸ assigned an infrared absorption to the Cd···H₂O complex.

The role of the binding of Hg²⁺ and HgOH⁺ in biochemical systems,^{19–21} and its adsorption into soil material²² have both recently been investigated, although it was not clear which

* To whom correspondence should be addressed.

[†] Department of Chemistry, University of Durham. E-mail: pavel.soldan@durham.ac.uk.

[‡] Department of Applied Biology and Chemical Technology, Hong Kong Polytechnic University.

[§] Department of Chemistry, University of Southampton. E-mail: E.P.Lee@soton.ac.uk.

^{||} Spectroscopy of Complexes and Radicals (SOCAR) Group, Department of Chemistry, School of Chemistry, Physics and Environmental Science, University of Sussex. E-mail: T. G.Wright@sussex.ac.uk. Fax: +44 1273 677196.

electronic state had been considered in each case. We also note in passing that the reactions of model II–VI precursor Group IIb hydrides with water have been studied computationally²³—it is not implausible that in such systems, especially at higher temperatures and if plasmas are employed, that cationic species, such as HgOH^+ may be of importance.

The stability of $\text{M}^{2+}\cdot\text{H}_2\text{O}$ complexes has recently been the subject of some controversy in the literature, with recent attention focused on the $\text{Cu}^{2+}\cdot\text{H}_2\text{O}$ complex. Stace et al.²⁴ commented that the 1:1 complex between Cu^{2+} and H_2O was not stable, and that the smallest number of water molecules required to stabilize the Cu^{2+} dication was three; in the case of less than three waters, charge transfer would occur. This claim was refuted by El-Nahas,²⁵ who had calculated²⁶ the 1:1 complex to be stable. Subsequently, two groups published experimental evidence that in fact the 1:1 complexes can be observed experimentally.^{27,28} In ref 12, we discussed some of the interesting points regarding the observability of $\text{M}^{2+}\cdot\text{H}_2\text{O}$ complexes, and we summarize some of these at the end of this work.

II. Theoretical Details

Owing to the large number of electrons for Hg, we employed effective core potentials (ECPs). We then augment the ECP with a large, flexible valence space that contains polarization and diffuse functions. The precise nature of the valence basis set is determined in Hartree–Fock (HF) calculations, where the underlying, contracted part of the valence basis set is selected such that the resulting wave function “behaves well”, by which we mean that it does not have sudden jumps in the contraction coefficients (indicative of gaps in the basis set)—which necessitates the use of sufficient basis functions, covering the whole valence region. The simplest way of designing such a basis set is via even-tempered sets, where the center and ratio are altered in the light of the calculated wave function. Once the contracted [spd] part of the basis set is designed, then the polarization and diffuse functions are added heuristically in the light of the underlying basis set, based on previous experience, and the resulting wave functions.

The first basis set employs the LANL2 ECP,²⁹ to which is normally added a double- ζ valence basis set; here, we remove that basis set and add our own—designed, as outlined in Appendix 1. This yields a LANL2[9s7p7d4f] basis set for Hg; for H_2O , a 6-311++G(3df,3pd) basis set was employed, giving a total number of basis functions of 168—we denote these basis sets simply by LANL2 below.

The second basis set employs the ECP60MWB ECP³⁰ (where the M indicates that the neutral atom is used in the derivation of the ECP and WB implies the use of the quasirelativistic approach described by Wood and Boring³¹), which treats up until the 4p shell as core, with the $5s^2 5p^6 5d^{10} 6s^2$ electrons as valence. It is described in Appendix 1. This yields a ECP60MWB[10s8p7d4f] basis set for Hg; for H_2O , a 6-311++G(3df,3pd) basis set was employed, giving a total number of basis functions of 172. We denote these simply as ECP60MWB-1 in the below.

The above two basis sets were used for geometry optimizations at the B3LYP, MP2 and QCISD levels of theory in the cases of $\text{Hg}\cdot\text{H}_2\text{O}$ and $\text{Hg}^{2+}\cdot\text{H}_2\text{O}$ and at the UMP2, CASSCF,^{32,33} CASSCF+MP2,³⁴ RCCSD,³⁵ and RCCSD(T)³⁶ levels for HgOH^+ . (U)MP2, B3LYP, and QCISD calculations were performed employing Gaussian98.³⁷ For the CASSCF, CASSCF+MP2, RCCSD, and RCCSD(T) calculations, MOLPRO³⁸ was employed. In all MP2, QCISD, and CCSD(T)

TABLE 1: Calculated Ionization Energies (eV) of Mercury at CCSD(T)/ECP60MWB[11s10p8d5f4g] Level

method	$\text{Hg} \rightarrow \text{Hg}^+ + e^-$	$\text{Hg} \rightarrow \text{Hg}^{2+} + 2e^-$
CCSD(T, freeze 5s5p)		26.974
CSSD	10.188	28.736
CCSD(T)	10.370	29.042
expt ³⁹	10.438	29.189

calculations, only the 1s orbital on O was kept frozen; for the CASSCF calculations, the oxygen 1s orbital was included in the active space as well.

In addition, single-point RCCSD(T) calculations were carried out to obtain energy differences to a greater accuracy; for these, the ECP60MWB ECP was again employed, but with a larger valence basis set, described in Appendix 1. This yields a ECP60MWB[11s10p8d5f4g] basis set for Hg; for H_2O , the aug-cc-pVQZ basis set was employed, giving a total number of basis functions of 324. We denote these as ECP60MWB-2 in the below.

III. Results and Discussion

(a) Ionization Energies. The ionization energies were calculated for the processes: $\text{Hg} \rightarrow \text{Hg}^+ + e^-$ and $\text{Hg} \rightarrow \text{Hg}^{2+} + 2e^-$ using the largest basis set, ECP60MWB-2. The results are given in Table 1 and compared to the values from Moore.³⁹ As may be seen, the agreement between the calculated values and the experimental ones is very good, which indicates that this basis set should be reliable for calculating energetics for Hg and Hg^{2+} . It should be noted that it is only when the 5s and 5p electrons are correlated that an accurate ionization energy is obtained, and that consequently we correlate these electrons for calculating reliable energetics below.

The calculated ionization energies reported herein compare very favorably with a recent set of relativistic coupled-cluster calculations.⁴⁰

(b) Optimized Geometries and Vibrational Frequencies.

(i) $\text{Hg}\cdot\text{H}_2\text{O}$. Three geometries were considered for the neutral complex: the two C_{2v} structures corresponding to the Hg interacting along the C_2 axis of H_2O , either with the O atom, denoted $\text{Hg}\cdot\text{OH}_2$, or the two H atoms, denoted $\text{Hg}\cdot\text{H}_2\text{O}$; and a C_s structure where the Hg atom interacts with just one H atom, denoted $\text{Hg}\cdot\text{HOH}$. The results are presented in Table 2. As may be seen, at the MP2 level, only the C_s configuration is a minimum, with the two C_{2v} geometries being saddle points, in agreement with our recent work on $\text{Cd}\cdot\text{H}_2\text{O}$ ¹², the imaginary frequency suggests a movement of the Hg atom in-plane, and so nonplanar structures were not considered for these orientations. A favoring of this geometry may be explained in terms of a competition between the dipole/induced dipole interaction, which would lead to the Hg being positioned along the C_2 axis, and the repulsion between the electrons of O and Hg, or between those of Hg and the two H atoms. If the latter is important, then we expect a geometry with the Hg interacting with the H atoms to be more stable than the one with the Hg atom interacting with O, which has more electrons. One must then rationalize why the C_s structure is lower in energy than the C_{2v} structure. Again, electron–electron repulsion will explain such a preference because in the C_s orientation, only the 1s electron of one H is present. It is clear, however, that the energy difference between all three of these structures is not great, and that many aspects of the interaction potential are likely to play a role in determining the final energy ordering. This is emphasized at the QCISD level, where the energy difference between the two C_{2v} structures has narrowed to almost zero,

TABLE 2: Geometry Optimization and Harmonic Frequency Calculations for Hg·H₂O with the LANL2[9s7p6d4f] Basis Set for Hg

	MP2		B3LYP		QCISD	
	LANL2	ECP60MWB	LANL2	ECP60MWB	LANL2	ECP60MWB
Hg..HOH C _s ^a						
Hg..H/Å	2.7536	2.7650	3.1309	3.0110	3.0849	3.0227
OH/Å	0.9607;0.9594	0.9606; 0.9593	0.9626; 0.9613	0.9625;0.9612	0.9576; 0.9573	0.9577; 0.9572
HgHO/°	178.7	178.9	178.9	178.2	178.6	175.5
HOH/°	103.9	103.9	105.0	105.0	104.3	104.3
rel. E _v /cm ⁻¹	0.0		0.0		0.0	
vib. freq. /cm ⁻¹	67a'; 106a'; 173a''; 1622a'; 3842a'; 3965a'	64a'; 112a'; 180a''; 1623a'; 3843a'; 3966a'	52a'; 119a'; 172a''; 1627a'; 3795a'; 3897a'	51a';105a';154a''; 1625a'; 3796a'; 3898a'		
Hg.H ₂ O C _{2v}						
	LANL2		LANL2		LANL2	
Hg..H/Å	3.1845		3.8758		3.5666	
OH/Å	0.9595		0.9613		0.9573	
HOH/°	103.5		104.9		104.3	
vib. freq. /cm ⁻¹	99ib ₂ ; 57a ₁ ; 119b ₁ ; 1619a ₁ ; 3861a ₁ ; 3975b ₂		45ib ₂ ; 33a ₁ ; 49b ₁ ; 1626a ₁ ; 3812a ₁ ; 3910b ₂			
rel. E _v /cm ⁻¹	92.3		59.8		36.9	
Hg.OH ₂ C _{2v}	LANL2		LANL2		LANL2	
Hg..O/Å	3.4221		3.8835		3.6372	
OH/Å	0.9595		0.9613		0.9574	
HOH/°	104.1		105.1		104.4	
vib. freq. /cm ⁻¹	70ib ₂ ; 41b ₁ ; 51a ₁ ; 1622a ₁ ; 3859a ₁ ; 3980b ₂		60ib ₁ ; 16b ₂ ; 23a ₁ ; 1626a ₁ ; 3811a ₁ ; 3911b ₂			
rel. E _v /cm ⁻¹	176.5		81.6		36.5	

^a All the optimized structures are slightly trans, except the B3LYP/ECP60MWB one, which is very slightly cis.

and the gap between the C_{2v} and the C_s structures has decreased considerably.

We then re-optimized the C_s geometry, and the results are also given in Table 2 at the MP2, B3LYP, and QCISD levels of theory using both the LANL2 basis set, and the ECP60MWB-1 basis set. As may be seen, the intermolecular bond lengths increase between the MP2 and the QCISD levels of theory, suggesting that a more complete description of electron correlation is leading to a greater contribution of the electron-electron repulsion between the electrons of the Hg and those of H₂O. From the results for the C_s structure, the B3LYP method seems to be intermediate between the MP2 and QCISD results, but veering much more toward the accuracy of the QCISD results than the MP2. This is interesting, as usually our experience is that the commonly used functionals in density functional theory (DFT) do not work very well for neutral complexes, and indeed even for cationic complexes can sometimes not be too good. However, when one looks at the C_{2v} results, it is clear that the B3LYP method is underestimating the interaction, giving a significantly longer Hg···H or Hg···O bond length. In addition, it may be seen that the intramolecular frequencies of the H₂O moiety agree rather well with the MP2 ones, but that the intermolecular ones are significantly lower. Thus, overall, the B3LYP method cannot be judged to be performing well for the neutral complex.

Comparing results at the same level of theory, but using the different basis sets, it can be seen that very similar results are obtained, suggesting that, as far as describing the geometry of the Hg·H₂O complex is concerned, both basis sets (and hence ECPs) are performing relatively well; that said, for energetics, as noted above when discussing the calculated ionization

energies of Hg, we anticipate that the ECP60MWB basis sets will be superior, owing to the correlation of the 5s and 5p electrons.

We note that recently, Guo and Goodings⁴¹ studied the Sc + H₂O system, and although they considered a Sc···H₂O complex, they only appear to have considered the scandium interacting with the oxygen, and not with the hydrogens. As noted previously¹² in the case of Cd···H₂O, both orientations of attachment of the H₂O by Cd led to minima. We also noted therein, and in the above, that the commonly used functionals for DFT studies do not seem to be wholly reliable for neutral complexes. Prior to that study, Zhang et al. had also looked at the Sc/H₂O system⁴² using the B3LYP method, and again appear not to have considered H-bonded structures. In our previous work,¹² we noted that there has been a review⁴³ of the spectroscopy and bonding of Groups I, IIA and IIIB complexes, but that it appeared that in none of the cases had interaction with the hydrogens been considered.

(ii) Hg²⁺·H₂O. For Cd²⁺·H₂O¹² and for all other M²⁺·H₂O 1:1 complexes (vide infra), to the authors' knowledge, the global minimum is with the M²⁺ interacting with the oxygen atom of H₂O: both planar and nonplanar structures are considered here for Hg²⁺·H₂O. The results of these optimizations are given in Table 3. As may be seen, at the B3LYP and MP2 levels of theory, the planar structure was a saddle point; and the nonplanar structure was a minimum. The energy difference between these two structures was very small (~0.1 kcal mol⁻¹), and so it is not possible to say from this level of theory, which of the two structures is the minimum. CCSD(T) calculations were then performed employing the larger ECP60MWB-2 basis set, with the results being given in Tables 4 and 5 (further discussion on these calculations will be presented below). As may be seen,

TABLE 3: Optimized Geometries and Harmonic Vibrational Frequencies for $\text{Hg}^{2+}\cdot\text{H}_2\text{O}$, C_{2v} (planar) and C_s (nonplanar)

	MP2		B3LYP		QCISD	
	LANL2	ECP60MWB	LANL2	ECP60MWB	LANL2	ECP60MWB
$\text{Hg}(\text{OH})_2^{2+}$ C_{2v} planar						
Hg...O/Å	2.0979		2.1794			2.0739
OH/Å	0.9745		0.9771			0.9745
HOH/°	109.9		110.2			111.2
δ^a/\circ	0		0			
vib. freq. /cm ⁻¹	239i(b ₁); 468a ₁ ; 743b ₂ ; 1602a ₁ ; 3609a ₁ ; 3705b ₂		311i(b ₁); 406a ₁ ; 715b ₂ ; 1606a ₁ ; 3600a ₁ ; 3682b ₂			
$E_{\text{rel}}^b/\text{cm}^{-1}$	48		92			174
$\text{Hg}(\text{OH})_2^{2+}$ C_s non-planar						
	LANL2	ECP60MWB	LANL2	ECP60MWB	LANL2	ECP60MWB
Hg...O/Å	2.1099	2.0656	2.1982	2.1289	2.1317	2.0939
OH/Å	0.9794	0.9818	0.9794	0.9850	0.9761	0.9782
HOH/°	108.3	108.7	108.3	108.8	108.3	108.5
δ^a/\circ	28.9	31.3	28.6	38.3	29.4	33.6
vib. freq. /cm ⁻¹	375a'; 466a'; 786a''; 1605a'; 3585a'; 3676a''	427a'; 497a'; 838a''; 1604a'; 3551a'; 3642a''	355a'; 460a'; 752a''; 1612a'; 3577a'; 3652a''	407a'; 608a'; 842a''; 1594a'; 3592a'; 3579a''		

^a δ is the angle between HgO and the C_2 axis of H_2O . ^b With respect to the corresponding nonplanar structure in bottom half of table.

TABLE 4: Calculated Binding Energies and BSSE for Non-Planar $\text{Hg}^{2+}\cdot\text{H}_2\text{O}$ at the CCSD(T)/ECP60MWB-2//QCISD/ECP60MWB-1 Level of Theory

	MP2	CCSD	CCSD(T)
E_g/E_h	-228.723 54	-228.700 286	-228.728 829
BSSE(H_2O)/kcal·mol ⁻¹	0.14	0.11	0.12
BSSE(Hg)/kcal·mol ⁻¹	1.84	1.70	1.81
BSSE _{tot} /kcal·mol ⁻¹	1.98	1.81	1.93
$\Delta E_g/\text{kcal}\cdot\text{mol}^{-1}$	93.5	89.8	92.1
$\Delta E_c(\text{CP})/\text{kcal}\cdot\text{mol}^{-1}$	91.5	88.0	90.2

TABLE 5: Calculated Binding Energies and BSSE for Planar $\text{Hg}^{2+}\cdot\text{H}_2\text{O}$ at the CCSD(T)/ECP60MWB-2//QCISD/ECP60MWB-1 Level of Theory

	MP2	CCSD	CCSD(T)
E_g/E_h	-228.723403	-228.700199	-228.728205
rel. E_g/cm^{-1}	31	19	137
$\Delta E_c(\text{CP})/\text{kcal}\cdot\text{mole}^{-1}$	91.6	88.1	90.1
rel. $\Delta E_c(\text{CP})^a/\text{cm}^{-1}$	-38	-43	66

^a With respect to nonplanar C_s $\text{Hg}(\text{OH})_2^{2+}$ (Table 4) at the corresponding level of calculation.

even the results of these high-level calculations are not definitive, with the CCSD results indicating that the planar structure is the lower in energy, whereas the CCSD(T) results indicate that the nonplanar one is; but in both cases, the difference in energy is minimal. The only safe conclusion is that $\text{Hg}^{2+}\cdot\text{H}_2\text{O}$ is quasi-planar, with a low bending potential, confirmed by the low vibrational frequency. In some ways, this nonplanar structure is reminiscent of the hydronium ion, H_3O^+ .

Looking at other studies, recently El-Nahas has studied a number of $\text{M}^{2+}\cdot\text{H}_2\text{O}$ complexes,^{26,44,45} using B3LYP and CCSD(T) methods, and found the minimum energy structures to be planar, with the M^{2+} interacting with the oxygen. This conclusion matched our own¹² regarding $\text{Cd}^{2+}\cdot\text{H}_2\text{O}$. This planar structure is as one would expect from an electrostatic picture, with the charge-dipole interaction dominating. In contrast, in the present work, we find that the nonplanar $\text{Hg}^{2+}\cdot\text{H}_2\text{O}$ structure is marginally more stable than the planar one. Analysis of the wave function indicates that covalency is of importance in $\text{Hg}^{2+}\cdot\text{H}_2\text{O}$, and a covalent interaction will favor a pyramidal structure. This covalency is inferred from the wave function, which indicates that there is involvement of the Hg d orbitals in the

TABLE 6: Calculated Binding Energies and BSSE for $\text{Hg}(\text{HOH})$ Using the ECP60MWB-2 Basis Set

	MP2	CCSD	CCSD(T)
E_g/E_h	-229.662715	-229.615977	-229.652069
BSSE(H_2O)/cm ⁻¹	12.4	10.1	10.9
BSSE(Hg)/cm ⁻¹	164.2	142.1	155.7
BSSE _{tot} /cm ⁻¹	176.6	152.7	166.6
$\Delta E_g/\text{cm}^{-1}$	498.8	295.2	379.8
$\Delta E_c(\text{CP})/\text{cm}^{-1}$	322.2	142.4	213.2

two HOMOs (4a'' and 10a''), with the major involvement being in the 4a'' orbital: this orbital loosely corresponds to $\text{O}p_y$, with some involvement of the H1s orbitals, as well as the Hg d orbital contribution. The very small energy difference between planar and nonplanar structures for this complex suggests that there is a fine balance between these two modes of interaction.

(c) Binding Energies. (i) $\text{Hg}\cdot(\text{H}_2\text{O})$. In Table 6 are shown the results of CCSD(T)/ECP60MWB-2//QCISD/LANL2 single-point energy calculations on the C_s structure of $\text{Hg}\cdot\text{HOH}$, including the BSSE, calculated via the full-counterpoise correction. The binding energy is sensitive to the level of theory, and it is clear that both CCSD and triples affect the binding energy relative to the MP2 method substantially, but in different directions. This sensitivity was expected from the relative energy changes noted in the above (see also Table 3).

With complexes containing heavy atoms, BSSE is always a difficult problem, owing to the large number of electrons, and the fact that for the inner valence electrons, very small admixtures of the ligand orbitals can potentially give a large relative energy. We have discussed this in our previous work on $\text{Cd}^{2+}\cdot\text{H}_2\text{O}$ and $\text{Cd}\cdot\text{H}_2\text{O}$,¹² $\text{Rg}\cdot\text{NO}$,^{46,47} and $\text{Rn}\cdot\text{H}_2\text{O}$.⁴⁸ For cationic species, the relative effect is much smaller, since the magnitude of the binding energy is much larger; the largest fractional error is with the neutral species. As noted in our previous work, we believe one has to consider the amount of BSSE *per electron*, and that a final value $< 10 \text{ cm}^{-1}$ is a good achievement. For $\text{Hg}\cdot\text{HOH}$, the total BSSE at the CCSD(T) level of theory is 167 cm^{-1} , which is 44% of the uncorrected binding energy. This is equivalent to $< 5 \text{ cm}^{-1}$ per electron, which is satisfactory. Thus, our best value for the monohydration energy of a Hg atom is 213 cm^{-1} , but it is not possible to estimate an error on this value.

(ii) $Hg^{2+}\cdot H_2O$. The calculated binding energies and BSSE are given in Table 4 for the nonplanar C_s O-bonded Hg²⁺·OH₂ structure. As may be seen, although the BSSE is larger—owing to the stronger interaction, shorter bond length and so greater overlap between the ligand and Hg²⁺ orbitals—the percentage of the binding energy is much smaller, at only 2% of the uncorrected value. An additional observation is that the level of theory is much less important here as the charge-dipole interaction becomes much more important.

In Table 5 are shown the binding energy data for the planar structure. The energy relative to the nonplanar structure is seen to be very small, being 137 cm⁻¹ at the CCSD(T) level before correction for BSSE. After correction for BSSE, this difference is slightly smaller at 66 cm⁻¹, but really, these differences are very small, emphasising the floppy nature of the complex.

Our best value for monohydration energy of Hg²⁺, after correction for BSSE, is thus 90 kcal mol⁻¹ (~31 500 cm⁻¹; 3.9 eV). This value is smaller than the value of 110 kcal mol⁻¹ obtained by Sinha,¹⁵ who used a semiempirical approach, but the agreement is reasonable, given the approximations in the former method. Probst¹⁴ used Hartree–Fock calculations, employing a DZ+P type basis set only, and obtained a value of 74 kcal mol⁻¹, which is clearly too small. The interaction energy for Hg²⁺·H₂O calculated using a point charge for the Hg²⁺ gave a value¹⁴ of 87.4 kcal mol⁻¹, which is in surprisingly good agreement with the value obtained herein.

(d) Reaction Hg²⁺ + H₂O → HgOH⁺ + H⁺. Reaction (1) is the simplest version of the hydration reaction of Hg²⁺; of course, in reality, there will be bulk solvent, as well as counteranions involved in the process. However, it is important, from a fundamental point of view to have an understanding of the isolated reaction 1, such as might occur in the gas phase under single-collision conditions.

The first question that requires addressing is as follows: What is the ground electronic state of HgOH⁺?

(i) $HgOH^+$. To our knowledge, HgOH⁺ has not been much studied. One can imagine two limits for the binding in this species: the charge separated Hg²⁺·OH⁻ or the charge-transferred species, Hg⁺·OH.

In a simple single-reference model, Hg²⁺·OH⁻ is expected to be a closed-shell, linear ¹Σ⁺ state or a bent ¹A' species. On the other hand, Hg⁺·OH in the ionic limit, is expected to have an unpaired electron in the Hg 6s orbital, and an open-shell π³ OH moiety. From these, one may expect ^{1,3}Π states, with the triplet state expected to be the lower. Upon bending, the triplet state will split into two ³A' or ³A'' under the influence of the Renner–Teller effect, and similarly for the ¹Π state.

In Table 7, we present the results of optimizations using the ECP60MWB-1 basis set employing various levels of theory. We also present the results of second derivative calculations at the UMP2 level. Note that the open-shell MP2 optimizations were performed employing unrestricted wave functions: the spin-contamination was negligible for the triplets, but for the open-shell singlets, which cannot be described in terms of a single restricted wave function, the spin-contamination was significant, as expected, with ⟨S²⟩ ≈ 1 rather than the expected 0. The MP2 energies cited are those obtained after two stages of spin-annihilation, where the ⟨S²⟩ values are much closer to the expected zero value. As can be seen from Table 7, however, CASSCF+MP2 optimizations gave similar results to the UMP2 optimizations.

The lowest state may be seen from Table 7 to be a bent ¹A' state, denoted \tilde{X}^1A' hereafter, which correlates to the ¹Σ⁺ state.

CASSCF and CASSCF+MP2 results were also performed in order to investigate the effects of multireference behavior; this was found to be small, as expected from the small value for the T₁ diagnostic,⁴⁹ calculated in the CCSD(T) calculations. The natural orbitals, obtained from the CASSCF calculations on the \tilde{X}^1A' state indicate that the 9a, 4a'', and 10a' HOMOs contain a significant amount of Hg 5d and 6s character. These HOMO orbitals correlate to the OH⁻ s and p orbitals. Consequently, we conclude that bending allows an increased interaction between the OH orbitals and the 5d and 6s orbitals on Hg as a result of the lower symmetry and their energetic proximity. Note that although a Mulliken population analysis indicated that the linear ¹Σ⁺ state is almost wholly Hg²⁺·OH⁻, the natural orbitals present a different picture with a significant involvement of the 5d orbitals of Hg involved in the bonding, both in σ and π orbitals. We note that if the 5d orbitals were not included explicitly, then of course this feature would be missed. Upon bending, the energy of this state lowers significantly; looking at the natural orbitals again, one may see that again the 5d orbitals are involved, and in fact interaction occurs between the OH π orbitals and the Hg 5d orbitals. The interaction appears to allow a sharing of charge, and so a lowering of the charge density on any one atom. The observation that a bent geometry is lower in energy than the linear one, and the wave function analysis, both point to the fact that covalent effects are important in the ground state. If the interaction between Hg²⁺ and OH⁻ were solely electrostatic, then we would expect a linear molecule, owing to the charge-dipole interaction.

The ³Π state also shows an imaginary π vibrational frequency at the UMP2 level (note that the π vibrational frequencies are nondegenerate, a frequent observation, attributable to a combination of numerical second derivatives and spin-contamination). As noted above, bending the ³Π state leads to the breaking of the orbital degeneracy, and the arising of ³A' and ³A'' states. Geometry optimization of the latter led back to the ³Π state both at the UMP2 and CASSCF levels, whereas the former led to a minimum, as shown in Table 7. This is a classic picture of a reasonably strong Renner–Teller interaction.⁵⁰ Regarding the corresponding ¹Π state, again a (split) imaginary π vibrational frequency was calculated, with the ¹A'' component being a minimum. We attempted both UMP2 and CASSCF calculations on the ¹A' component, but these calculations always converged to the \tilde{X}^1A' state; we expect this component to have a linear geometry, by comparison with the behavior of the ³A'' component of the ³Π state.

To obtain more reliable relative energies, we performed additional CCSD/ECP60MWB-2 and CCSD(T)/ECP60MWB-2 calculations at the CCSD(T)/ECP60MWB-1 optimized geometries. The results are given in Table 8. These suggest that the \tilde{X}^1A' state has a sizable barrier to linearity of 1.4 eV, while that of the ³A' state is much smaller at 0.11 eV.

Role of Electron Correlation. A very interesting observation arose during this work regarding the role of electron correlation. If one looks at the RHF energies that are the reference energies for the RCCSD(T) calculations, then the energy ordering is ³Π < ³A' < \tilde{X}^1A' < ¹Σ⁺. So it is the correlation energy that leads to the change in ordering of these states, see Table 7, and leads to the singlet state lowering its energy significantly more than the triplet ones. Also at the R(O)HF/ECP60MWB-1 level of theory, the triplet state has a linear minimum. These general observations occur at the MP2, CASSCF, MRCI, and RCCSD levels of theory, showing that even the lowest level of inclusion of electron correlation energy appears to get the ordering correct.

TABLE 7: Calculated Geometries and Vibrational Frequencies for HgOH⁺ Employing ECP60MWB-1 Basis Set

	(U)MP2 ^a	CASSCF	CASSCF-MP2	RCCSD	RCCSD(T)
¹ Σ ⁺					
HgO/Å	1.8570	1.8872	1.8531	1.8664	1.8682
OH/Å	0.9627	0.9400	0.9616	0.9549	0.9579
HgOH/°	180.0	180.0	180.0	180.0	180.0
freq./cm ⁻¹	1327iπ; 748.5σ; 3852σ				
E _{tot} /E _h	-228.415780	-227.611761	-228.4258204	-228.394132	-228.418159
¹ A'					
HgO/Å	1.9668	2.1015	1.9948	1.9757	1.9949
OH/Å	0.9808	0.9538	0.9770	0.9703	0.9746
HgOH/°	104.6	108.0	106.3	107.2	106.6
freq./cm ⁻¹	555a'; 1076a'; 3636a'				
E _{tot} /E _h	-228.470316	-227.684309	-228.483910	-228.443772	-228.472107
³ Π					
HgO/Å	2.4585	2.6186	2.4406	2.4779	2.4586
OH/Å	0.9727	0.9545	0.9738	0.9722	0.9747
HgOH/°	180.0	180.0	180.0	180.0	180.0
freq./cm ⁻¹	341iπ; 518π; 203σ; 3758σ				
E _{tot} /E _h	-228.430902	-227.669082	-228.449095	-228.418395	-228.436832
	⟨S ² ⟩ = 2.01 (2.00)				
³ A''					
HgO/Å	2.4121	2.5916	2.3982	2.4313	2.4128
OH/Å	0.9766	0.9552	0.9776	0.9767	0.9799
HgOH/°	123.3	143.4	123.8	123.4	121.2
freq./cm ⁻¹	232a'; 467a'; 3713a'				
E _{tot} /E _h	-228.434570	-227.671039	-228.453080	-228.421967	-228.441202
	⟨S ² ⟩ = 2.01 (2.00)				
¹ Π					
HgO/Å	2.5166	2.7077	2.5375		
OH/Å	0.9722	0.9538	0.9729		
HgOH/°	180.0	180.0	180.0		
freq./cm ⁻¹	267iπ; 78π; 184σ; 3765σ				
E _{tot} /E _h	-228.437890	-227.668796	-228.445397		
	⟨S ² ⟩ = 1.01 (0.07)				
¹ A''					
HgO/Å	2.4751	2.6904	2.5002		
OH/Å	0.9745	0.9543	0.9747		
HgOH/°	130.1	153.4	132.9		
freq./cm ⁻¹	200a'; 385a'; 3741a'				
E _{tot} /E _h	-228.438878	-227.668796	-228.447235		
	⟨S ² ⟩ = 1.01 (0.07)				

^a For open-shell species, UMP2 was employed to obtain the optimized geometries, but the energies are PUMP2. The ⟨S²⟩ values given are the unprojected (UMP2) values first, followed by the second annihilated values (PUMP2) in parentheses. Note that spin contamination is large for the open-shell singlets, as expected.

TABLE 8: CCSD(T)/ECP60MWB-2//CCSD(T)/ECP60MWB-1 Energies for HgOH⁺

state	E _{CCSD(T)/E_h}	E _{rel./eV}
¹ A'	-228.638451	0
¹ Σ ⁺	-228.586782	1.41
³ A''	-228.601338	1.01
³ Π	-228.597128	1.12

TABLE 9: CCSD(T)/ECP60MWB-2 Energies for Species Involved in Reaction 1

species	E _{CCSD(T)/E_h}	ZPVE/cm ⁻¹ (eV)
Hg ²⁺	-152.219462	0
H ₂ O	-76.363581	4504 (0.56)
HgOH ⁺ (X̃ ¹ A')	-228.638451	2634 (0.33)
H ⁺	0	0

(ii) ΔH_r for Reaction 1 and the Observability of Hg²⁺·H₂O. In Table 9 are presented the RCCSD(T)/ECP60MWB-2 energies for the relevant species. From these, it is straightforward to calculate ΔH_r for reaction 1 as -1.74 eV (-40.0 kcal mol⁻¹), exothermic, as expected. Consequently, were one able to create a reasonable number of Hg²⁺ dications in the gas phase and react them with water molecules, one would expect to be able to see product HgOH⁺ formed. Of course, this conclusion is

only based upon thermodynamical considerations, and ideally one would need to investigate kinetic stability by investigating the heights of barriers during the reaction. We expect there to be no barrier to be associated with the initial Hg²⁺ + H₂O reaction, leading to the complex, but there to be a barrier between the complex and the HgOH⁺ + H⁺ products. Whether this barrier is significant for the kinetics or not will depend on its magnitude, and the internal energy of the species involved.

Finally, we consider the observability of Hg²⁺·H₂O. As we noted above, and in more detail in our previous paper¹² on Cd²⁺·H₂O, it is really the preparation of the species that is important. It is clear that the species will be stable, if there is a barrier to charge transfer. This barrier is certainly there, since it is facile to calculate that the Hg⁺ + H₂O⁺ asymptote is lower in energy than the Hg²⁺·H₂O one, and so there must exist a curve crossing between the Hg²⁺·H₂O curve, and a curve correlating to the Hg⁺ + H₂O⁺ asymptote. Because charge-transfer can occur, the species are thermodynamically unstable, but kinetically they can exist and be observable. The critical thing is the lifetime of the states: Schröder et al.²⁷ estimate the lifetimes to be of the order of microseconds at the very least for Cu²⁺·H₂O. This lifetime clearly depends on the internal energy of the M²⁺·H₂O,

and so if Hg²⁺·H₂O can be formed with very little excitation energy, one can envisage that these would be the most favorable conditions under which to observe the dicationic complex. One obvious route to achieve this would be photoionization; however, as we pointed out before,¹² that the neutral species appears to have a very different equilibrium geometry from the cation would seem to preclude this. (It is also worth pointing out that conclusions regarding stability of cations obtained via photoionization need to be made cautiously, since the stability of the *neutrals* is also crucial.) Of course, if the molecule really is very floppy at the zero-point level, then the vibrational wave function may be delocalized enough to allow observable Franck–Condon factors for the ionization to the M²⁺·OH₂ minimum. The methods of charge-stripping²⁷ and electrospray ionization²⁸ are the alternative methods of preparation of M²⁺·H₂O that were used in the case of Cu²⁺·H₂O.

IV. Conclusions

We have calculated enthalpies for the monohydration of Hg⁰ and Hg²⁺. For the neutral species, even state-of-the-art methods are challenged by this species, but a reasonably accurate binding energy is obtained, and this is small, as expected. Contrary to many previous studies, we find that (as in our previous work on a number of species), the lowest energy isomer is with the Hg interacting with the hydrogen atoms of water, in an asymmetric C_s orientation. As far as we can tell, these previous studies do not appear to have considered this mode of binding. The idea of an equilibrium geometry is, however, rather nebulous because the species is floppy, and so the mercury atom samples a wide range of space.

For the dication, in contrast, the interaction is very strong, and the Hg²⁺ is positioned on the O atom. Interestingly, we find that the lowest energy orientation is actually nonplanar (although the barrier to linearity is very small), and we attribute this to covalency in the binding, which is supported by an analysis of the natural orbitals.

We also have determined the ground-state symmetry of the HgOH⁺ species for the first time, and find it to be a bent, closed-shell ¹A' state. The barrier to linearity is significant, and is attributed to a sizable covalency that allows the charge density on the mercury and OH to be lowered. Higher in energy are a ³Π and ¹Π state, but both are split by a reasonably strong Renner–Teller interaction.

Finally, we conclude that Hg²⁺·H₂O will be kinetically stable in the gas phase, owing to a barrier to charge-transfer, but that it is not thermodynamically stable. Its observability will depend to a large extent on the method by which the dication is prepared.

Acknowledgment. The authors are grateful to the EPSRC for the award of computer time at the Rutherford Appleton Laboratories under the auspices of the United Kingdom Computational Chemistry Working Party (UKCCWP), which enabled these calculations to be performed. E.P.F.L. is grateful to the Research Grant Council (RGC) of the Hong Kong Special Administration Region (HKSAR) and the Research Committee of the Hong Kong Polytechnic University for support. P.S. would like to thank the EPSRC for his present funding at Durham (Senior Research Assistantship). T.G.W. is grateful to the EPSRC for the award of an Advanced Fellowship. Useful discussions with Prof. A. J. Stace (Sussex) are acknowledged.

Appendix 1

The “LANL2” basis set is described below.

The LANL2 ECP describes all electrons up until the 5p orbital, and so only the 5d¹⁰6s² electrons for Hg are valence. The contracted [sd] part of the valence basis set was obtained from a HF calculation on Hg and consisted of thirteen s functions ($\zeta = 10.0-0.002\ 441\ 4$, ratio = 2.0) and 10 d functions ($\zeta = 10.0-0.019\ 531\ 2$, ratio = 2.0). To this were added the following uncontracted functions:

- eight s: $\zeta = 0.8-0.001\ 310\ 72$, ratio = 2.5;
- seven p: $\zeta = 1.1-0.002\ 543\ 29$, ratio = 2.75;
- six d: $\zeta = 2.0-0.009\ 750\ 79$, ratio = 2.9;
- four f: $\zeta = 1.5-0.034\ 985\ 4$, ratio = 3.5.

The ECP60MWB-1 basis set is described below.

The contracted [2s1p1d] functions were obtained from a HF calculation on Hg as before, but in this case, two contracted s functions were derived, corresponding to the 5s and 6s orbitals. The uncontracted basis set employed for the latter calculations consisted of seventeen s functions (center $\zeta = 1.0$, ratio = 2.0), fifteen p functions (center $\zeta = 1.0$, ratio = 2.0) and eleven d functions (center $\zeta = 1.0$, ratio = 1.8). To this were added the following uncontracted functions:

- eight s: $\zeta = 12.0-0.00889354$, ratio = 2.8;
- seven p: $\zeta = 5.0-0.0103758$, ratio = 2.8;
- six d: $\zeta = 2.0-0.00975079$, ratio = 2.9;
- four f: $\zeta = 1.5-0.0349854$, ratio = 3.5.

The ECP60MWB-2 basis set for Hg is described below.

The ECP60MWB ECP was again utilized, but with a larger valence basis set. The contracted [2s1p1d] functions from the ECP60MWB basis set were again employed, with the uncontracted part of the basis set being increased to the following:

- nine s: center $\zeta = 0.2$, ratio = 2.75;
- nine p: center $\zeta = 0.2$, ratio = 2.75;
- seven d: center $\zeta = 0.2$, ratio = 2.5;
- five f: center $\zeta = 0.4$, ratio = 3.5;
- four g: $\zeta = 3.0-0.046875$, ratio = 4.0.

References and Notes

- (1) Slemr, F. In *NATO ASI Ser. 2 Environment Vol. 21*; Baeyens, W., Ebinghaus, R., Vasiliev, O., Eds.; Kluwer Academic Publishers: Dordrecht, The Netherlands, 1996; 33–84.
- (2) Carpi, A. *Water Air Soil Pollut.* **1997**, *98*, 241.
- (3) Horne, P. A.; Williams, P. T. *Waste Management* **1996**, *16*, 579.
- (4) Slemr, F.; Schuster, G.; Seiler, W. *J. Atm. Chem.* **1985**, *3*, 407.
- (5) Schroeder, W. H.; Yarwood, G.; Niki, H. *Water Air Soil Pollut.* **1991**, *56*, 653.
- (6) Lindberg, S. E.; Stratton, W. J. *Environ. Sci. Technol.* **1998**, *32*, 49.
- (7) Lindberg, S.; Landis, M. S.; Stevens, R. K.; Brooks, S. *Atm. Environ.* **2001**, *35*, 5377.
- (8) Schroeder, W. H.; Munthe, J.; Lindqvist, O. *Water Air Soil Pollut.* **1989**, *48*, 337.
- (9) Ebinghaus, R.; Kock, H. H.; Temme, C.; Einax, J. W.; Löwe, A. G.; Richter, A.; Burrows, J. P.; Schroeder, W. H. *Environ. Sci. Technol.* **2002**, *36*, 1238.
- (10) Lindberg, S. E.; Brooks, S.; Lin, C.-J.; Scott, K. J.; Landis, M. S.; Stevens, R. K.; Goodsite, M.; Richter, A. *Environ. Sci. Technol.* **2002**, *36*, 1245.
- (11) Cotton, F. A.; Wilkinson, G. *Advanced Inorganic Chemistry*; Wiley: Chichester, 1980.
- (12) Lee, E. P. F.; Soldán, P.; Wright, T. G. *J. Phys. Chem. A* **2001**, *105*, 8510.
- (13) Hancock, R. D.; Marsicano, F. *J. Chem. Soc., Dalton Trans.* **1976**, 1832.
- (14) Probst, M. M. *J. Mol. Struct. (THEOCHEM)* **1992**, *253*, 275.
- (15) Sinha, S. P. *Inorg. React. Mech.* **2000**, *2*, 33.
- (16) Rudolph, W. W.; Pye, C. C. *J. Phys. Chem. B* **1998**, *102*, 3564.
- (17) Rudolph, W. W.; Pye, C. C. *Phys. Chem. Chem. Phys.* **1999**, *1*, 4583.
- (18) Greene, T. M.; Brown, W.; Andrews, L.; Downs, A. J.; Chertihin, G. V.; Runeberg, N.; Pyykkö, P. *J. Phys. Chem.* **1995**, *99*, 7925.
- (19) Ferreira, M. L.; Gschaider, M. E. *Macromol. Biosci.* **2000**, *1*, 233.
- (20) Šponer, J.; Burda, J. V.; Sabat, M.; Leszczynski, J.; Hobza, P. *J. Phys. Chem. B* **1998**, *102*, 5951.

- (21) Šponer, J.; Sabat, M.; Burda, J. V.; Leszczynski, J.; Hobza, P. *J. Phys. Chem. B* **1999**, *103*, 2528.
- (22) Sarkar, D.; Essington, M. E.; Misra, K. C. *Soil Sci. Soc. Am. J.* **2000**, *64*, 1968.
- (23) Cundari, T. R.; Fu, W. T. *Int. J. Quantum Chem.* **1999**, *71*, 47.
- (24) Stace, A. J.; Walker, N. R.; Wright, R. R.; Firth, S. *Chem. Phys. Lett.* **2000**, *329*, 173.
- (25) El-Nahas, A. M. *Chem. Phys. Lett.* **2000**, *329*, 176.
- (26) El-Nahas, A. M.; Tajima, N.; Hirao, K. *Chem. Phys. Lett.* **2000**, *318*, 333.
- (27) Schröder, D.; Schwarz, H.; Wu, J.; Wesdemiotis, C. *Chem. Phys. Lett.* **2001**, *343*, 258.
- (28) Stone, J. A.; Vukomanovic, D. *Chem. Phys. Lett.* **2001**, *346*, 419.
- (29) Hay, P. J.; Wadt, W. R. *J. Chem. Phys.* **1985**, *82*, 270.
- (30) Andrae, D.; Häussermann, U.; Dolg, M.; Stoll, H.; Preuss, H. *Theor. Chim. Acta* **1990**, *77*, 123.
- (31) Wood, J. H.; Boring, A. M. *Phys. Rev. B*, **1978**, *18*, 2701.
- (32) Werner, H.-J.; Knowles, P. J. *J. Chem. Phys.* **1985**, *82*, 5053.
- (33) Knowles, P. J.; Werner, H.-J. *Chem. Phys. Lett.* **1985**, *115*, 259.
- (34) Celani, P.; Werner, H.-J. *J. Chem. Phys.* **2000**, *112*, 5546.
- (35) Hampel, C.; Peterson, K.; Werner, H.-J. *Chem. Phys. Lett.* **1992**, *190*, 1.
- (36) Knowles, P. J.; Hampel, C.; Werner, H.-J. *J. Chem. Phys.* **1993**, *99*, 5219. *Erratum*: Knowles, P. J.; Hampel, C.; Werner, H.-J. *J. Chem. Phys.* **2000**, *112*, 3106.
- (37) Frisch, M. J.; Trucks, G. W.; Schlegel, H. B.; Scuseria, G. E.; Robb, M. A.; Cheeseman, J. R.; Zakrzewski, V. G.; Montgomery, J. A., Jr.; Stratmann, R. E.; Burant, J. C.; Dapprich, S.; Millam, J. M.; Daniels, A. D.; Kudin, K. N.; Strain, M. C.; Farkas, O.; Tomasi, J.; Barone, V.; Cossi, M.; Cammi, R.; Mennucci, B.; Pomelli, C.; Adamo, C.; Clifford, S.; Ochterski, J.; Petersson, G. A.; Ayala, P. Y.; Cui, Q.; Morokuma, K.; Malick, D. K.; Rabuck, A. D.; Raghavachari, K.; Foresman, J. B.; Cioslowski, J.; Ortiz, J. V.; Stefanov, B. B.; Liu, G.; Liashenko, A.; Piskorz, P.; Komaromi, I.; Gomperts, R.; Martin, R. L.; Fox, D. J.; Keith, T.; Al-Laham, M. A.; Peng, C. Y.; Nanayakkara, A.; Gonzalez, C.; Challacombe, M.; Gill, P. M. W.; Johnson, B. G.; Chen, W.; Wong, M. W.; Andres, J. L.; Head-Gordon, M.; Replogle, E. S.; Pople, J. A. *Gaussian 98*; Gaussian, Inc.: Pittsburgh, PA, 1998.
- (38) MOLPRO is a package of ab initio programs written by Werner, H.-J.; Knowles, P. J. with contributions from J. Almlöf, J.; Amos, R. D.; Berning, A.; Deegan, M. J. O.; Eckert, F.; Elbert, S. T.; Hampel, C.; Lindh, R.; Meyer, M.; Nicklass, A.; Peterson, K.; Pitzer, R.; Stone, A. J.; Taylor, P. R.; Mura, M. E.; Pulay, P.; Schuetz, M.; Stoll, H.; Thorsteinsson, T.; Cooper, D. L.
- (39) Moore, C. E. *Atomic Energy Levels*, Natl. Bur. Stand. (U. S.) Circ. 467 (US, GPO, Washington, DC, 1958).
- (40) Eliav, E.; Kaldor, U.; Ishikawa, Y. *Phys. Rev. A*, **1995**, *52*, 2765.
- (41) Guo, J.; Goodings, J. M. *Chem. Phys. Lett.* **2001**, *342*, 169.
- (42) Zhang, L.; Dong, J.; Zhou, M. *J. Phys. Chem. A* **2000**, *104*, 8882.
- (43) Fuke, K.; Hashimoto, J.; Iwata, S. *Adv. Chem. Phys.* **1999**, *110*, 431.
- (44) El-Nahas, A. M. *Chem. Phys. Lett.* **2001**, *345*, 325.
- (45) El-Nahas, A. M. *Chem. Phys. Lett.* **2001**, *348*, 483.
- (46) Lee, E. P. F.; Soldán, P.; Wright, T. G. *J. Phys. Chem. A* **1998**, *102*, 6858.
- (47) Lee, E. P. F.; Gamblin, S. D.; Wright, T. G. *Chem. Phys. Lett.* **2000**, *322*, 377.
- (48) Lee, E. P. F.; Wright, T. G. *J. Phys. Chem. A* **1999**, *103*, 7843.
- (49) Lee, T. J.; Taylor, P. R. *Int. J. Quantum Chem.* **1989**, *S23*, 23.
- (50) Herzberg, G. *Molecular Spectra and Molecular Structure III: Electronic Spectra and Electronic Structure of Polyatomic Molecules*; Krieger: Malabar, FL, 1991.